

The Structures and Biological Activities of the Lipo-oligosaccharide Nodulation Signals Produced by Type I and II Strains of *Bradyrhizobium japonicum**

(Received for publication, April 2, 1993)

Russell W. Carlson‡§, Juan Sanjuan¶, U. Ramadas Bhat‡, John Glushka‡, Herman P. Spaink||, Andre H. M. Wijfjes||, Anton A. N. van Brussell||, Thomas J. W. Stokkermans**, N. Kent Peters**, and Gary Stacey¶

From the ‡Complex Carbohydrate Research Center, University of Georgia, Athens, Georgia 30602-4712, the ¶Department of Microbiology and the Center for Legume Research, University of Tennessee, Knoxville, Tennessee 37996, the ||Institute of Molecular Plant Sciences, Leiden University, 2311 VJ Leiden, The Netherlands, and the **Ohio State Biotechnology Center, Ohio State University, Columbus, Ohio 43210

***Bradyrhizobium japonicum* produces lipo-oligosaccharide signal molecules that induce deformation of root hairs and meristematic activity on soybeans. *B. japonicum* USDA135 (a Type I strain) produces modified chitin pentasaccharide molecules with either a terminal *N*-C_{16:0} or *N*-C_{18:1}-glucosamine with and without an *O*-acetyl group at C-6 and with 2-*O*-methylfucose linked to C-6 of the reducing *N*-acetylglucosamine. An additional molecule has *N*-C_{16:1}-glucosamine and no *O*-acetyl group. All of these molecules cause root hair deformation on *Vicia sativa* and *Glycine soja*. The C_{18:1}-containing molecules were tested and found to induce meristem formation on *G. soja*. USDA61 (a Type II strain) produces eight additional molecules. Five have a carbamoyl group on the terminal *N*-acylglucosamine. Six have chitin tetrasaccharide backbones. Three have a terminal *N*-acyl-*N*-methylglucosaminosyl residue. In four molecules, the reducing-end *N*-acetylglucosamine is glycosidically linked to glycerol and has a branching fucosyl, rather than a 2-*O*-methylfucosyl, residue. One molecule has a terminal *N*-acylglucosamine that has both acetyl and carbamoyl groups (one each).**

Bacteria belonging to the genera *Rhizobium*, *Bradyrhizobium*, and *Azorhizobium* are able to establish symbiotic relationships with leguminous plants by infecting their roots. This relationship results in the formation of root nodules that contain the nitrogen-fixing microsymbiont. Nodule formation requires the exchange of signal molecules between the *Rhizobium* symbiont and the legume host. The *nodD* gene product together with flavonoids produced by the host legume, isoflavones in the case of soybean (4, 5), activate the transcription of rhizobial genes that are required for nodulation, *i.e.* the *nod* genes (1-3). The result is the synthesis of lipo-oligosaccharides (also referred to as Nod metabolites) that cause root hair deformation and cortical cell division on the legume host root (3, 6-10).

* This work was supported in part by United States Department of Energy Grants DE-FG09-37ER13810 (to the Complex Carbohydrate Research Center) and 92ER20072 (to G. S.), National Institutes of Health Grant GM39583 (to R. W. C.), National Science Foundation Grant DCB8819422 (to N. K. P.), a Royal Netherlands Academy of Arts and Sciences grant (to H. P. S.), a Fulbright postdoctoral fellowship (to J. S.), and NATO Grant G10188 (to H. P. S., G. S., and R. W. C.). The costs of publication of this article were defrayed in part by the payment of page charges. This article must therefore be hereby marked "advertisement" in accordance with 18 U.S.C. Section 1734 solely to indicate this fact.

§ To whom correspondence should be addressed: Complex Carbohydrate Research Center, University of Georgia, 220 Riverbend Rd., Athens, GA 30602-4712. Tel.: 706-542-4401; Fax: 706-542-4412.

These lipo-oligosaccharides are *N*-fatty acylated chitin oligomers. The *nod* genes that determine host specificity dictate variations in the type of *N*-acyl substituent present on the terminal glucosamine and in substituents that are present on the reducing *N*-acetylglucosamine. The terminal *N*-acylglucosamine can also be acetylated at C-6. A single species of *Rhizobium* can produce several lipo-oligosaccharides. In the case of *Rhizobium meliloti*, the major lipo-oligosaccharide is a tetramer with hexadecadienoic acid (C_{16:2}) as the *N*-acyl substituent and a sulfate group at C-6 of the reducing *N*-acetylglucosamine. This molecule has been designated as NodRm-IV(C_{16:2},S) (8) after the nomenclature of Spaink *et al.* (6). The terminal *N*-acylglucosamine is frequently acetylated at C-6 and is designated as NodRm-IV(Ac,C_{16:2},S) (11). Minor amounts of lipotri- and tetrasaccharides containing hexadecanoic (C_{16:0}), hexadecenoic (C_{16:1}), or hexadecatrienoic (C_{16:3}) acid have also been reported for *R. meliloti* (9). The unsaturated fatty acyl residue and the sulfate group are required for the specific interaction with *Medicago* (8). *Rhizobium leguminosarum* bv. *viciae* produces a lipo-pentasaccharide in which the terminal *N*-acylglucosamine contains octadecatetraenoic acid (C_{18:4}) as the acyl substituent and is acetylated at C-6 (6). There are no substitutions on the reducing *N*-acetylglucosamine. Both the C_{18:4} and the *O*-acetyl substituents are required for the specific interaction with the legume host (6). Enzymes that are involved in the synthesis or addition of these substituents are encoded by the host specificity genes *nodEF* (required for the synthesis of C_{18:4}) and *nodL* (required for *O*-acetylation) (6). Lipotetrasaccharides, rather than pentasaccharides, that contain vaccenic acid (C_{18:1Δ¹¹}) as the *N*-acyl substituent are also synthesized by *R. leguminosarum* bv. *viciae* (6).

The above lipo-oligosaccharides are all from *Rhizobium* species that have a symbiotic relationship with hosts that form indeterminate nodules. Hosts such as soybean and bean form determinate nodules. The differences between these two types of nodules have been described in a recent review (12). *B. japonicum* strains are symbionts of soybean, but can also have other hosts, such as siratro. Our previous report (7) showed that *B. japonicum* USDA110 produces one major lipo-oligosaccharide; however, as detected by thin-layer chromatography (14), *B. japonicum* strain USDA135 produces several lipo-oligosaccharides. The USDA110 lipo-oligosaccharide has a pentasaccharide backbone that contains octadecenoic acid (C_{18:1}) as the *N*-acyl substituent and a 2-*O*-methylfucosyl residue at C-6 of the reducing *N*-acetylglucosamine and is designated as NodBj-V(C_{18:1},MeFuc) (7). The structures of the USDA135 Nod metabolites are described in this report. Another report describes the structures of a family of lipo-oligosaccharides from the broad host range (which includes soybean) *Rhizobium* sp.

NGR234 (13). This strain produces lipo-oligosaccharides having pentasaccharide backbones with C_{18:1Δ11} as the *N*-acyl substituent and a 2-*O*-methylfucose at C-6 of the reducing *N*-acetylglucosamine. The 2-*O*-methylfucosyl residue can also be sulfated or acetylated. In addition, the *N*-acylglucosamine is also *N*-methylated and contains either none, one, or two carbamoyl groups at C-3, C-4, and/or C-6. A similar *N*-methylated monocarbamoylated Nod metabolite has also been isolated from *Azorhizobium caulinodans*; however, this metabolite contains *D*-arabinose, rather than 2-*O*-methylfucose, linked to C-6 of the reducing *N*-acetylglucosamine (45).

The *B. japonicum* species is divided into two major groups with both *B. japonicum* USDA110 and USDA135 members of the Type I strains. Type II strains are quite different from Type I strains with regard to their DNA homology and the type of extracellular polysaccharide produced and also in that they belong to the cowpea miscellany and therefore may have a broader host range than Type I strains (15). To understand the differences in the ability of Type I and II strains to nodulate different hosts, it is necessary to determine the structural differences between the lipo-oligosaccharides produced by these strains. In this report, we describe the structures and biological activities of several lipo-oligosaccharides from *B. japonicum* USDA135 (a Type I strain) and the structures of the lipo-oligosaccharides from strain USDA61 (a Type II strain).

EXPERIMENTAL PROCEDURES

Bacterial Strains and Growth Conditions—*B. japonicum* strains were maintained on *Rhizobium* defined yeast extract (RDY) agar as described (16). The cells were grown in liquid RDY medium at 30 °C until the cultures reached an A₆₀₀ of 0.5–0.6. The cells were then washed and diluted to an A₆₀₀ of 0.1 in minimal medium (17) containing glycerol as the carbon source and sodium glutamate as the nitrogen source. Seed extract (*Glycine max* cv. Essex or Williams) or genistein (2 μM final concentration) (5) was added, and the bacteria were grown at 30 °C for an additional 40 h. Strains used were the wild-type *B. japonicum* USDA135, USDA110, and USDA61 (18).

Detection of Lipo-oligosaccharides by Thin-layer Chromatography (14)—Cells were grown in liquid RDY medium at 30 °C until the cultures reached an A₆₀₀ of 0.5–0.6. Bacteria were pelleted in a microcentrifuge, washed once with liquid minimal medium, and diluted in this medium to an A₆₀₀ of 0.1. Cells were then induced by the addition of 2 μM genistein or soybean seed extract. At the time of genistein or root exudate addition, 50 μCi of [¹⁴C]acetate (56 mCi/mmol, 1 Ci = 37 GBq; ICN) was added, and the cultures were incubated overnight. The induction of the nodulation genes was indirectly monitored by the induction of β-galactosidase in a strain containing a *nodY-lacZ* fusion (i.e. ZB977) (19). Supernatants of labeled cultures were extracted with 1-butanol and applied to octadecyl silica TLC plates (Sigma) as described (14). Plates were dried and exposed to x-ray film (Kodak X-Omat AR) for 2–6 days at room temperature.

Purification of Lipo-oligosaccharides—The Nod metabolites were purified as described previously (7). The cells were pelleted, and the supernatants were extracted with 0.33 volume of distilled 1-butanol. The butanol layer was collected, and the butanol was removed by rotary evaporation. The residue was resuspended in acetonitrile:water (1:1) and chromatographed using 60% acetonitrile:water on a Silica Gel 60 column (1.6 × 100 cm; Pharmacia LKB Biotechnology Inc.). Fractions containing Nod metabolites were further analyzed and purified by HPLC¹ using a Pharmacia SuperPac Pep-S column (5 μm, 5 × 250 mm). The eluent from the HPLC column was monitored at 206 nm.

Assay for Biological Activity of Nod Metabolites—Seeds of *Glycine soja* PI468397 were surface-sterilized and germinated as previously described (16). Cortical cell division activity was tested following the spot inoculation method originally described by Turgeon and Bauer (20). Two-day-old seedlings were placed in plastic pouches containing 5

ml of plant nutrient solution (16) and allowed to grow overnight in the dark. At the time of inoculation, the position of the smallest emergent root hairs, visible in a dissecting microscope at magnification × 50, and the root tip were marked on the top face of the plastic pouch. The top face of the plastic pouch was slit with a razor blade and rolled back to expose the root. Prior to inoculation, a single Amberlite bead was transferred with forceps to a position above the root tip ~80% of the distance between the root tip and the smallest emergent root hairs. Droplets containing different amounts of purified Nod metabolites in a volume of 30–50 nl were delivered by micropipette to the same position as the Amberlite bead. The droplets were allowed to dry on the root surface for 10–15 min, and the pouches were taped closed. To avoid undesirable binding of Nod metabolites to the plastic, a sterile straw was placed next to the root to hold the plastic at a distance for the first 2 h after inoculation. Plants were then transferred to a plant growth room with a 16-h light/8-h dark photo period. Roots were analyzed for cortical cell division and nodule formation by following the clearing method described by Truchet *et al.* (21).

Hair deformation activity was determined as previously described using *Vicia sativa* subsp. *nigra* (6) or *G. soja* (7) as test plants.

Chemical Analysis of Lipo-oligosaccharides—Glycosyl composition analysis was performed by GC-MS analysis of alditol acetates prepared as described in York *et al.* (22). Glycosyl linkage analysis was performed by GC-MS analysis of partially methylated alditol acetates prepared by the procedure of Hakomori modified as described by York *et al.* (22). Analysis was performed using a 30-m SP2330 capillary column (Supelco, Inc.). Fatty acids were identified by GC-MS analysis of their methyl esters prepared by acid-catalyzed methanolysis (23) in methanolic 4 M HCl at 80 °C for 14 h. Fatty acids were also isolated by alkaline hydrolysis (1.7 M NaOH) in dimethyl sulfoxide at 80 °C for 14 h, followed by acidification and extraction into chloroform. Methyl esters of the fatty acids released by alkaline hydrolysis were prepared by methanolysis in methanolic 1 M HCl at 80 °C for 1 h. Analysis was performed using a 30-m capillary DB1 column (J & W Scientific). The fatty acyl residue that was attached to glucosamine was determined by mild methanolysis in dry methanolic 1 M HCl at 80 °C for 1 h, followed by trimethylsilylation and analysis by GC-MS using a 15-m DB1 column (8, 11, 25). The location of the double bond in the C_{18:1} fatty acyl residue was determined by the preparation and analysis of dimethyl disulfide ethers of the C_{18:1} methyl ester (26). The resulting products were identified by GC-MS using a DB1 column.

FAB-MS Analysis—FAB-MS was carried out on a VG-ZAB SE instrument at an accelerating voltage of 8 kV in the positive mode with thioglycerol (TG) or glycerol:*m*-nitrobenzyl alcohol (1:1) as the matrix. The samples were dissolved in dimethyl sulfoxide, and ~2–10 μg in 1 μl was applied to the probe. Tandem MS-MS analysis was performed using a JEOL HX110/HX110 mass spectrometer operated at 10-kV accelerating potential. Spectra acquired by MS-1 are averaged profile data as recorded by a JEOL complement data system. These spectra were acquired from *m/z* 0 to 3000 at a rate that would scan from *m/z* 1 to 6000 in 1 min. A filtering rate of 300 Hz and an approximate resolution of 1500 were used in acquiring these spectra. Ions were produced by liquid secondary ion mass spectrometry. Collisionally induced dissociation was performed in the third field free region using helium as the collision gas. The helium pressure was sufficient to attenuate the primary ion beam by 75%, and the collision cell was floated at 3 kV. The samples were dissolved in dimethyl sulfoxide as described above. Glycerol:*m*-nitrobenzyl alcohol (1:1) was used as the matrix for the tandem MS-MS analyses.

NMR Analysis—Prior to analysis, the samples were suspended in ²H₂O and lyophilized. This process was repeated three times. All spectra were recorded on a Bruker AMX 600 MHz spectrometer using deuterated dimethyl sulfoxide as the solvent. Two-dimensional double quantum filtered COSY (27), TOCSY (28, 29), ROESY (30), and HSQC (31) data sets were collected in phase-sensitive mode using the time proportioned phase incrementation (32) method. In all experiments, low-power presaturation was applied to the residual HDO signal.

For the homonuclear experiments, typically 512 FIDs of 2048 complex data points were collected, with 64 scans/FID for the TOCSY data and 128 scans for the double quantum filtered COSY and ROESY data. The spectral width was set to 5000 Hz, and the carrier placed at the residual HDO peak. The TOCSY pulse program contained a 130-ms MLEV17 (33) spin-lock pulse, and the ROESY experiment used a 200-ms continuous wave spin-lock pulse flanked by two 90° pulses for offset compensation (34).

For the HSQC spectrum, 256 FIDs of 4096 complex points were acquired, with 256 scans/FID. The spectral width in the carbon dimension was set to 120 ppm, with the carrier at δ 70 referenced to dimethyl

¹ The abbreviations used are: HPLC, high pressure liquid chromatography; GC-MS, gas chromatography-mass spectrometry; FAB-MS, fast atom bombardment mass spectrometry; TG, thioglycerol; TOCSY, total correlation spectroscopy; ROESY, rotating frame nuclear Overhauser effect spectroscopy; HSQC, heteronuclear single quantum coherence; Cb, carbamoyl; Gro, glycerol; FID, free induction decay.

sulfoxide at δ 39.7 with respect to 2,2-dimethyl-2-silapentane-5-sulfonate. The GARP (35) sequence was used for ^{13}C decoupling during acquisition.

One-dimensional ROESY experiments used the following pulse sequence: selected 190° -selected 180° - t -acquired, where the selective pulses were calibrated DANTE (36) pulse trains. The exorcycle (37) phase cycle was applied to the selective 180° pulse. The selective 90° pulse was 8.9 ms, and the refocusing delay t was 5.6 ms. The continuous wave spin-lock pulse was 500 ms.

Data were processed typically with a lorentzian-to-gaussian weighting function applied to t_2 and a shifted squared sine bell function and zero filling applied to t_1 . Processing was performed with Felix software (Hare Research, Inc.).

RESULTS

Purification of *B. japonicum* Nod Metabolites—Fig. 1 shows a thin-layer chromatogram of the Nod metabolites from strains USDA110, USDA135, and USDA61. Strain USDA110 produced one major Nod metabolite, with trace amounts of several others, while strains USDA135 and USDA61 both produced several Nod metabolites. The Nod metabolites from the various strains were purified by HPLC. Fig. 2 shows the HPLC profile of the Nod metabolites from strain USDA135. Four fractions (F1–F4) were isolated, with fractions F3 and F4 present in the largest amounts. The identification of the various HPLC fractions was determined by TLC analysis. Because strain USDA135 produced larger amounts of fractions F3 and F4, they were characterized in the greatest detail. These results are described below.

Composition and Glycosyl Linkage Analysis—The glycosyl compositions of fractions F3 and F4 were determined by the preparation and GC-MS analysis of alditol acetates and trimethylsilyl methylglycosides. Both fractions F3 and F4 had a 1:5 ratio of 2-*O*-methylfucose to *N*-acetylglucosamine.

Methylation analysis of both fractions F3 and F4 gave a 1:3:1 ratio of terminal to 4-linked to 4,6-linked *N*-acetylglucosamines. Lower amounts of terminal 2-*O*-methylfucose were also detected. The lower value for the partially methylated alditol acetate of terminally linked 2-*O*-methylfucose was probably a result of some loss due to the volatility of its partially methylated alditol acetate.

The fatty acid components of both fractions F3 and F4 showed the presence of $\text{C}_{16:0}$, octadecanoic ($\text{C}_{18:0}$), and $\text{C}_{18:1}$ fatty acids. Since small amounts of $\text{C}_{16:0}$, $\text{C}_{18:0}$, and $\text{C}_{18:1}$ could be due to slight contamination by membrane phospholipids, it was necessary to identify those fatty acid residues that are part of the Nod factor preparations. Therefore, the fatty acyl components of fractions F3 and F4 were determined by mild methanolysis, preparation of trimethylsilyl ethers, and GC-MS analysis. This method was used since mild methanolysis readily liberates the methylglycoside of *N*-acylglucosamine and thus permits the identification of the fatty acyl moiety that is still attached to the glucosamine (8, 11, 25). Using this procedure, it

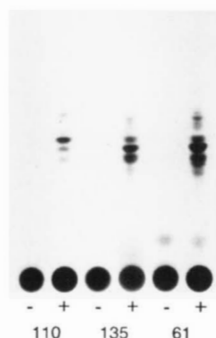


FIG. 1. Thin-layer chromatography of metabolites produced by wild-type strains USDA110, USDA135, and USDA61 in absence (-) or presence (+) of soybean seed extracts.

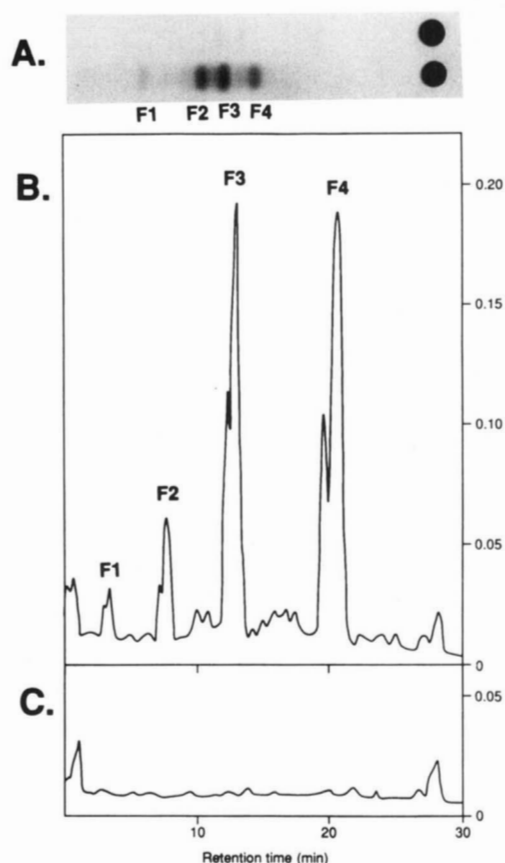


FIG. 2. Elution profile of reverse-phase HPLC purification of Nod metabolites from strain USDA135. A, TLC profile of the Nod metabolites. A comparison between uninduced and induced cultures is shown. B and C, HPLC profile of the Nod metabolites from induced and uninduced USDA135, respectively.

was found that fraction F3 contained both *N*-hexadecanoylglucosamine and *N*-octadecenoylglucosamine, while fraction F4 contained only *N*-octadecenoylglucosamine. The electron impact and chemical ionization spectra for the trimethylsilyl methylglycosides of these components are shown in Fig. 3. The $(\text{M} + \text{H})^+$ ions were at m/z 674 and 648 for the trimethylsilyl methylglycosides of *N*-octadecenoylglucosamine and *N*-hexadecanoylglucosamine, respectively (Fig. 3A). A fragment ion at m/z 204 (the fragment containing C-3 and C-4) was found for both *N*-acylglucosaminosyl residues, and the characteristic C(2)-C(3) fragment ions at m/z 395 and 369 were observed for *N*-octadecenoylglucosamine and *N*-hexadecanoylglucosamine, respectively (Fig. 3B). Other fragment ions were consistent with those reported for the trimethylsilyl derivatives of *N*-acylglucosamine methylglycosides (38). The presence of both *N*-hexadecanoylglucosamine and *N*-octadecenoylglucosamine in fraction F3 indicated that this fraction contained a mixture of at least two molecules, one with an *N*-hexadecanoyl substituent and the other with an *N*-octadecenoyl substituent.

Our previous paper (7) reported the location of the double bond in the $\text{C}_{18:1}$ fatty acyl substituent of NodBjV($\text{C}_{18:1}$,MeFuc) from strain USDA110 to be between carbons 9 and 10, *i.e.* oleic acid, while all other studies on $\text{C}_{18:1}$ -containing Nod metabolites reported the presence of $\text{C}_{18:1\Delta 11}$. Therefore, the location of the double bond in the $\text{C}_{18:1}$ present in fraction F4 was examined using methods that greatly increased the $\text{C}_{18:1}$ recovered from the Nod metabolite. Saponification with 1.7 M NaOH in dimethyl sulfoxide at 80°C for 14 h increased by 5–10 fold, over that previously reported (7), the amount of $\text{C}_{18:1}$ liberated from the Nod metabolite. However, when the temperature was increased to 100°C , the recovery of $\text{C}_{18:1}$ was greatly

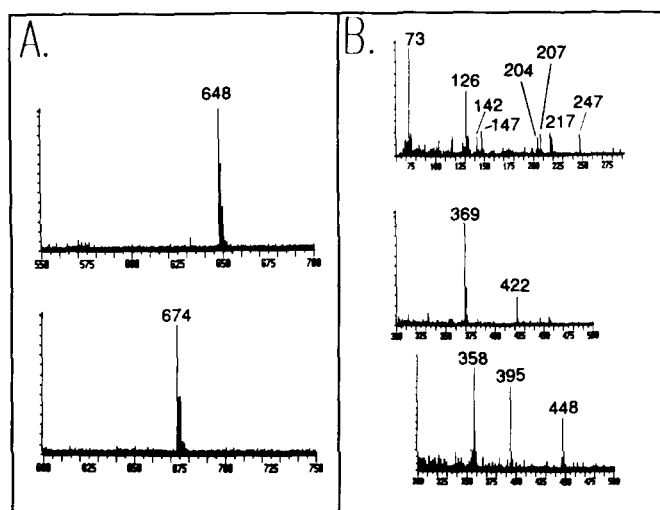


FIG. 3. Chemical ionization (A) and electron impact (B) mass spectra of trimethylsilyl methylglycosides of *N*-acetylglucosamine derivatives from USDA135 fractions F3 and F4 in which *N*-acyl substituent is either $C_{16:0}$ or $C_{18:1}$. In the electron impact mass spectra, the fragmentation pattern at m/z 60–300 are identical for both *N*-acetylglucosamine derivatives (B, top spectrum). The electron impact mass spectra (m/z 300–500) of the N - $C_{16:0}$ - and N - $C_{18:1}$ -acetylglucosamine derivatives are shown (B, middle and bottom spectra).

reduced. The release of $C_{18:1}$ from the Nod metabolites was also increased by performing methanolysis in methanolic 4 M (rather than 1 M) HCl at 80 °C for 14 h. The location of the double bond in the $C_{18:1}$ fatty acid released by these methods was determined by preparing the dimethyl disulfide derivatives of the fatty acid methyl esters (26). Analysis of this derivative by GC-MS (data not shown) gave mass fragments at m/z 145, 245, and 213. The ions at m/z 145 and 245 result from fragmentation between the carbons that carry the dimethyl disulfide groups and show that the double bond was between carbons 11 and 12. The fragment at m/z 213 is due to the loss of methanol (–32 atomic mass units) from the ion at m/z 245. Thus, the octadecenoyl component in this Nod metabolite is vaccenic acid. The fatty acyl component of the Nod metabolite from USDA110, previously identified as oleic acid (7), will be re-examined using the above methods to ensure greater release of the fatty acyl component from that Nod metabolite.

FAB-MS of Fractions F3 and F4—The FAB-MS spectra for fractions F3 and F4 are shown in Fig. 4 (A and B, respectively). The $(M + H)^+$ ions observed for fraction F4 were at m/z 1416 and 1458, with the ion at m/z 1458 being of greatest intensity. The ion at m/z 1416 is due to the presence of a small amount of non-*O*-acetylated (*i.e.* –42 atomic mass units) metabolite. It is likely that the presence of the non-*O*-acetylated metabolite in this fraction is due to the loss of this labile substituent during sample preparation. It should be noted that fraction F3, which contains the largest amount of this same non-*O*-acetylated molecule, is well separated from fraction F4 during HPLC purification (see Fig. 2). A TG adduct was observed for molecules carrying an unsaturated fatty acyl residue. Hence, the $(M + H + TG)^+$ ion, m/z 1566 (+108), is due to the TG adduct of fraction F4. Fragment ions at m/z 468 (present but not shown in Fig. 4), 671, 874, and 1077 and their TG adducts were also observed. The structure shown in Fig. 4 is consistent with this fragmentation pattern and with the chemical data described above. The ion at m/z 468 shows that the *O*-acetyl and *N*-octadecenoyl groups are present on the terminal glucosamine. The difference of 203 atomic mass units between fragment ions is consistent with a sequence of 3 additional *N*-acetylglucosaminosyl residues. The mass difference, 381 atomic mass units, between the

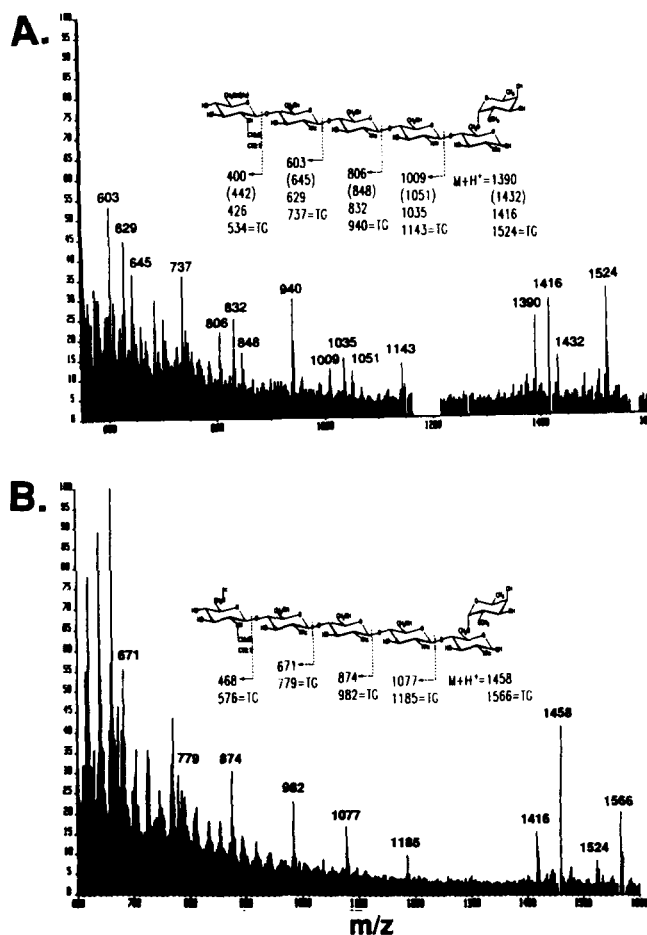


FIG. 4. FAB-MS spectra of USDA135 fractions F3 (A) and F4 (B).

$(M + H)^+$ ion (m/z 1458) and the largest fragment ion (m/z 1077) is due to the presence of a 2-*O*-methylfucosyl-*N*-acetylglucosamine disaccharide component at the reducing end of the molecule. The only branching glycosyl residue found during methylation analysis was a 4,6-linked *N*-acetylglucosamine (see above). Thus, it is likely that the terminal 2-*O*-methylfucosyl residue is linked to C-6 of the reducing *N*-acetylglucosamine. Confirmation of this linkage was obtained by two-dimensional NMR analysis and is discussed below. These data are consistent with fraction F4 being NodBj-V(Ac, $C_{18:1}$,MeFuc).

The FAB-MS spectrum of fraction F3 (Fig. 4A) shows that it consists of a mixture of three molecules. $(M + H)^+$ ions at m/z 1390 and 1432 are due to non-*O*-acetylated and *O*-acetylated molecules, respectively, with an *N*-hexadecenoyl substituent, *i.e.* NodBj-V($C_{16:0}$,MeFuc) and NodBj-V(Ac, $C_{16:0}$,MeFuc). The $(M + H)^+$ ion at m/z 1416 and its TG adduct at m/z 1524 are due to the non-*O*-acetylated molecule that contains an *N*-octadecenoyl substituent, NodBj-V($C_{18:1}$,MeFuc). The *O*-acetylated version of this molecule, which was the major component of fraction F4 (see above), was not found in fraction F3. Thus, fraction F3 consists of a mixture of three compounds: NodBj-V($C_{16:0}$,MeFuc), NodBj-V(Ac, $C_{16:0}$,MeFuc), and NodBj-V($C_{18:1}$,MeFuc). The presence of the trimethylsilyl methylglycosides of both *N*-octadecenoylglucosamine and *N*-hexadecenoylglucosamine in fraction F3 (described above) is also consistent with this fraction containing a mixture of these compounds. The presence of NodBj-V($C_{16:0}$,MeFuc) in fraction F3 is probably due to the loss of the labile *O*-acetyl group during sample preparation since fraction F2, which contains only NodBj-V($C_{16:0}$,MeFuc) (discussed below), was separated with base-

line resolution from fraction F3 (see Fig. 2).

The structures shown in Fig. 4 were confirmed by FAB-MS analysis of peracetylated or prerduced (with NaB^2H_4) and peracetylated fraction F3. The results are shown in Fig. 5 (A and B). Peracetylation without prerduction was done in dimethyl sulfoxide using *N*-methylimidazole as the catalyst (39). The FAB-MS spectrum of the peracetylated products of fraction F3 is shown in Fig. 5A. The fragment ions are consistent with the presence of a mixture of two peracetylated Nod metabolites, one containing an *N*-octadecenoyl substituent and the other an *N*-hexadecanoyl substituent. Also notice that both peracetylation products were present as *N*-methylimidazolium glycosides. Reduction (with NaB^2H_4) prior to peracetylation also resulted in a mixture of two reduced peracetylated Nod metabolites containing *N*-octadecenoyl and *N*-hexadecanoyl substituents (Fig. 5B). Additionally, prerduction of the reducing *N*-acetylglucosamine to an alditol prior to peracetylation prevented a reaction with the *N*-methylimidazole. The ions at m/z 1964 and 1904 are due to the loss of ketene and both ketene and acetic acid, respectively, from the $(M + H)^+$ molecule at m/z 2007. Similarly, the ion at m/z 1878 is due to the loss of both ketene and acetic acid from the $(M + H)^+$ molecule at m/z 1981. The FAB-MS spectrum in Fig. 5A was taken using TG as the matrix; therefore, TG adducts were observed for the $(M + H)^+$ ion of the *N*-octadecenoyl-containing molecule and all its fragment

ions. *m*-Nitrobenzyl alcohol was used as the matrix for the spectrum shown in Fig. 5B, and the TG adducts are noticeably absent.

FAB-MS analysis was also performed on fractions F1 and F2. Not enough of these fractions was obtained for a complete chemical or NMR analysis. Fraction F2 gave a spectrum (data not shown) that is consistent with this component being NodBj-V($\text{C}_{16:0}$,MeFuc), *i.e.* the $(M + H)^+$ ion at m/z 1390 and fragment ions at m/z 1009, 806, 603, and 400. The spectrum for fraction F1 (data not shown) gave the $(M + H)^+$ ion at m/z 1388, the $(M + H + \text{TG})^+$ ion at m/z 1496, and the $(M + \text{Na} + \text{TG})^+$ ion at m/z 1518. The presence of TG adducts indicates that this molecule contains an unsaturated fatty acyl substituent. Since the TG adducts often give more intense ions, the TG adduct of the fragment ion at m/z 1007, m/z 1115, was also observed. As with the other Nod metabolites, the difference between m/z 1496 and 1115 is 381 atomic mass units and is consistent with the reducing end of this molecule containing a 2-*O*-methylfucosyl-*N*-acetylglucosamine disaccharide component. An unsaturated fatty acyl substituent (which would give rise to TG adducts) that is consistent with the molecular size of this molecule is a hexadecenoyl substituent. Thus, it is proposed that this Nod metabolite is NodBj-V($\text{C}_{16:1}$,MeFuc). Fatty acid analysis of fraction F1 (data not shown) also showed the presence of hexadecenoic acid; however, not enough material was available to determine the location of the double bond.

NMR Analysis—The proton NMR spectrum of NodBj-V($\text{Ac},\text{C}_{18:1}$,MeFuc) is shown in Fig. 6. The resonance at δ 4.93 ($J_{1,2} = 2.4$ Hz) is consistent with that reported for the anomeric proton of the reducing α -*N*-acetylglucosamine of other Nod metabolites (6, 8, 11). The resonances between δ 4.34 and 4.50 ($J_{1,2} = 9$ Hz) are due to the anomeric protons of the β -linked *N*-acyl- and *N*-acetylglucosaminosyl residues as reported for other Nod metabolites (6, 8, 11). The resonance at δ 5.00 ($J_{1,2} = 3.7$ Hz) is consistent with an α -linked 2-*O*-methylfucosyl residue and is identical to that reported for the Nod metabolite from *B. japoni-*

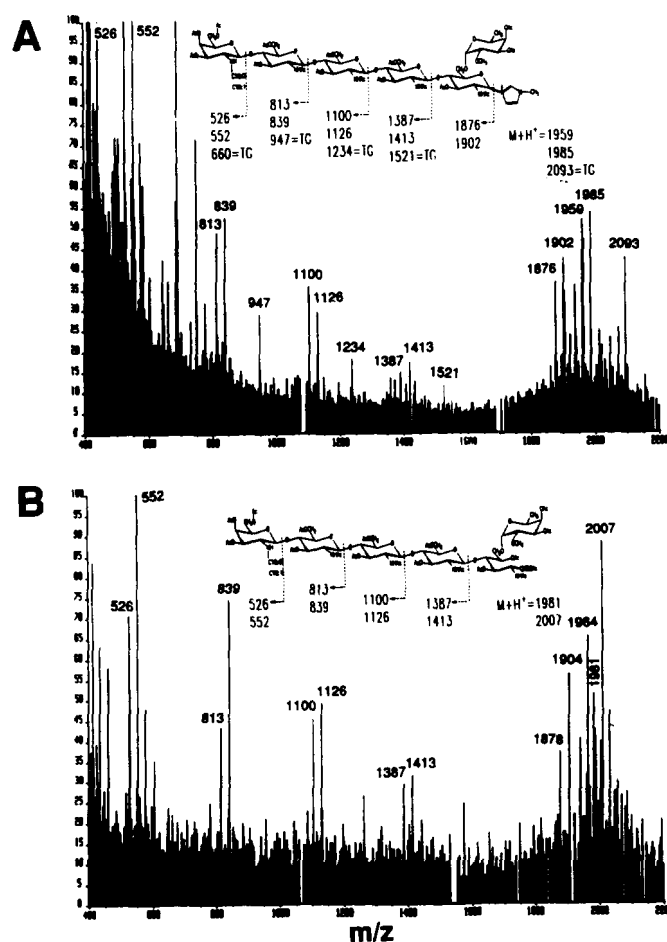


FIG. 5. FAB-MS spectra of peracetylated (A) and prerduced and peracetylated (B) USDA135 fraction F3. The matrix used for A was TG; thus, TG adducts are observed for the $\text{C}_{18:1}$ -containing metabolites. The matrix used for B was *m*-nitrobenzyl alcohol. In B, ions due to the loss of ketene (-42 atomic mass units), acetic acid (-60 atomic mass units), or both (-102 atomic mass units) from the molecular ions are also observed (m/z 1964 (2006 to 42), 1904 (1964 to 60), 1938 (1980 to 42), and 1878 (1938 to 60)).

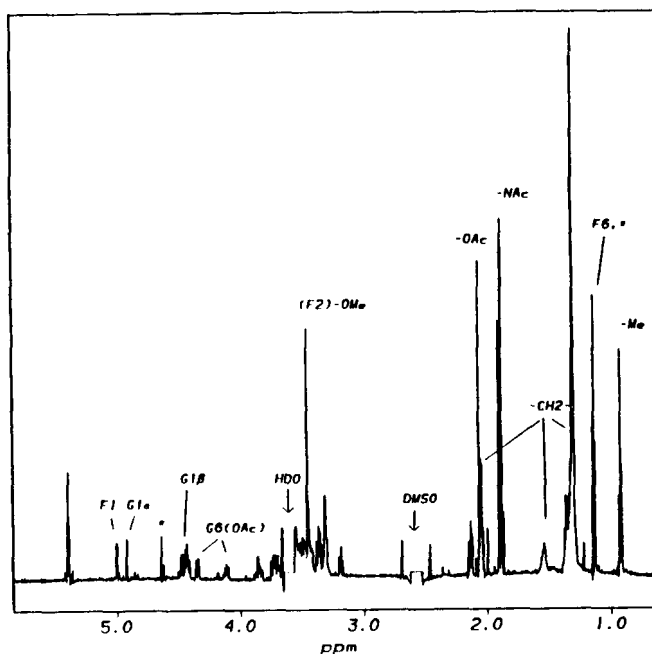


FIG. 6. Proton NMR spectrum of fraction F4 Nod metabolite from USDA135 (NodBj-V($\text{Ac},\text{C}_{18:1}$,MeFuc)). The resonances labeled with F are due to the 2-*O*-methylfucosyl residue, and those labeled with G to the *N*-acetylglucosamine. The resonances due to the methylene ($-\text{CH}_2-$) and methyl groups (Me) of the fatty acyl residue and to the *O*- and *N*-acetyl groups ($-\text{OAc}$ and $-\text{NAC}$, respectively) are as indicated. DMSO, dimethyl sulfoxide.

cum USDA110 (7). Because of the reducing *N*-acetylglucosamine, this Nod metabolite exists as a mixture of α/β -anomers; therefore, a second minor doublet at δ 4.98 is due to the 2-*O*-methylfucosyl residue attached to the reducing β -*N*-acetylglucosaminosyl residue of the anomeric mixture. The singlet at δ 3.46 is due to the methoxy protons of the 2-*O*-methylfucosyl residue, and the singlet of lower intensity at δ 3.44 is a second methoxy proton resonance due, again, to the anomeric effect of the reducing *N*-acetylglucosaminosyl residue. The resonance at δ 1.13 is due to the H-6 methyl protons of the 2-*O*-methylfucosyl residue.

A complete assignment of the 2-*O*-methylfucosyl protons was obtained by two-dimensional NMR analysis of NodBj-V(C_{18:1},MeFuc) (purified from strain USDA110) and NodBj-V(Ac,C_{18:1},MeFuc) (fraction F4 from USDA135). A two-dimensional TOCSY spectrum (data not shown) indicated a cross-peak between the 6-deoxymethyl protons and H-5 of the same residue. In addition, connectivity was also observed through H-2 (δ 3.37), H-3 (δ 3.74; $J_{3,2} = 10.2$ Hz, $J_{3,4} = 3.6$ Hz), and H-4 (δ 3.56). Connectivity from H-5 to H-4 was not seen due to the unfavorable gauche relationship of the protons. However, a two-dimensional ROESY spectrum (data not shown) showed the expected cross-peak from H-3 to H-5 as well as cross-peaks from H-1 and H-2 to the methoxy protons at δ 3.46. Additionally, an HSQC heterocorrelated spectrum of NodBj-V(C_{18:1},MeFuc) (Fig. 7D) showed that C-2 of the 2-*O*-methylfucosyl residue (labeled F2 in Fig. 7D) resonated significantly downfield (δ 81.9), which is characteristic of a substituted position (in this case, a methyl substituent). These NMR data are consistent with the presence of a 2-*O*-methylfucosyl residue and confirm the glycosyl composition and linkage data described above.

The linkage of the 2-*O*-methylfucosyl residue to C-6 of an *N*-acetylglucosaminosyl residue (known to be the reducing residue from the FAB-MS data described above) was confirmed by NMR analysis. An HSQC spectrum showed a set of cross-peaks (labeled G6 in Fig. 7D) at δ 68.7/ δ 3.65 and 3.82 corresponding to C-6/H-6 cross-peaks of an *N*-acetylglucosaminosyl residue and shifted downfield from the other C-6 atoms at δ 60–61. This 7–8-ppm downfield shift for C-6 is consistent with a glycosyl linkage at that position. Both one- and two-dimensional TOCSYs (data not shown) show that the two H-6 atoms (δ 3.65 and 3.82) that are coupled to this downfield C-6 belong to the reducing *N*-acetylglucosaminosyl residue. A selective one-dimensional ROESY experiment (Fig. 7C), in which the 2-*O*-methylfucosyl H-1 (δ 5.00) was irradiated, enhanced the upfield signal of one of these H-6 atoms (δ 3.65). Fig. 7 (A and B) shows that this H-6 is present in both NodBj-V(Ac,C_{18:1},MeFuc) and NodBj-V(C_{18:1},MeFuc), respectively. These data, together with the FAB-MS and methylation data described above, show that the 2-*O*-methylfucosyl residue is linked to C-6 of the reducing-end *N*-acetylglucosaminosyl residue.

The location of the *O*-acetyl group was also deduced from NMR analysis. The proton spectrum (Fig. 6) of NodBj-V(Ac,C_{18:1},MeFuc) shows a sharp singlet at δ 2.1 that is due to the *O*-acetylmethyl protons. The proton signals at δ 4.11 ($J_{5,6} = 7.7$ Hz, $J_{6,6} = 12.6$ Hz) and δ 4.35 ($J_{5,6} < 1$ Hz) are due to the terminal *N*-acylglucosamine H-6 atoms since they were shown by two-dimensional TOCSY (spectrum not shown) to be connected to the unique H-4 resonance (δ 3.18) of the terminal unsubstituted C-4 of this residue. The downfield position of these H-6 atoms is characteristic of an *O*-acetyl substitution. Therefore, these data, together with the FAB-MS data, show that the *O*-acetyl group of NodBj-V(Ac,C_{18:1},MeFuc) is at C-6 of the terminal *N*-acylglucosaminosyl residue.

The resonance at δ 5.40 (see Fig. 6) is due to the vinyl protons of the C_{18:1} fatty acyl component. The small H(9)-H(10) cou-

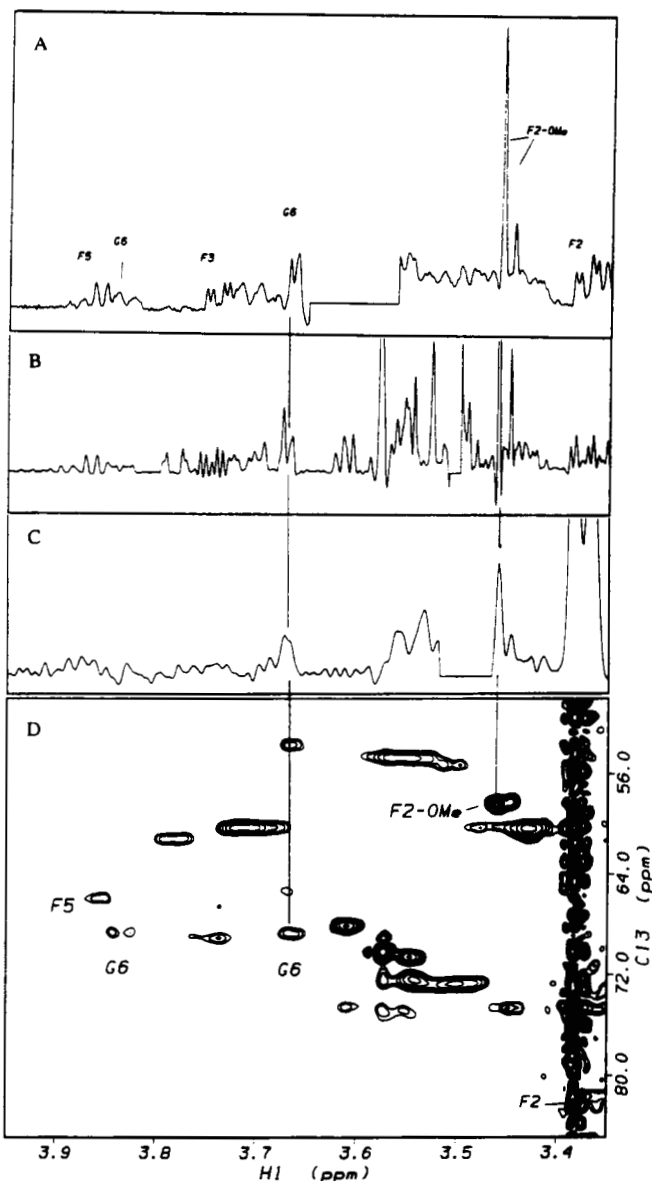


FIG. 7. A and B, one-dimensional proton spectra of NodBj-V(C_{18:1},MeFuc) and NodBj-V(Ac,C_{18:1},MeFuc), respectively; C, one-dimensional ROESY spectrum in which H-1 of the 2-*O*-methylfucosyl residue was irradiated; D, two-dimensional HSQC spectrum. Resonances labeled G6 are due to the C-6/H-6 cross-peaks of the reducing *N*-acetylglucosamine. Those resonances labeled F5, F2, and F2-OMe are due to the H-5, H-2, and methoxy protons, respectively, of the 2-*O*-methylfucosyl residue.

pling constant indicates a *cis*-configuration. Resonances typical for the methylene and methyl protons of the fatty acyl group are present as indicated in Fig. 6.

Analysis of Nod Metabolites from Strain USDA61—Small amounts of these metabolites were purified as described above. Four fractions were obtained. Analysis by FAB-MS (data not shown) showed that the first two fractions had (M + H)⁺ ions (and fragment ions) at *m/z* 1416 (426, 629, 832, and 1035) and 1458 (468, 671, 874, and 1077), respectively. In addition, the TG adducts of each ion were observed. These data are consistent with fraction F1 and fraction F2 being NodBj-V(C_{18:1},MeFuc) and NodBj-V(Ac,C_{18:1},MeFuc), respectively, the major metabolites found in USDA135 and whose structures are described above. FAB-MS analysis of fraction F2 also showed another (M + H)⁺ ion at *m/z* 1273 (with a TG adduct at *m/z* 1381). Fragment ions of correspondingly lower intensities were observed at

m/z 426, 629, and 832. No fragment ion at m/z 1035 was observed. These data, when compared with the structures described above for USDA135, indicated that this unidentified Nod metabolite consists of $\text{GlcN}(\text{C}_{18:1})\text{-GlcNAc-GlcNAc-R}$, where R has a mass of 440 (*i.e.* 1272 - 832). An additional minor $(\text{M} + \text{H})^+$ ion at m/z 1287 was also observed in fraction F2. The increase of 14 atomic mass units (*i.e.* 1287 - 1273) indicates that this minor component is a methylated version of the $(\text{M} + \text{H})^+$ molecule at m/z 1273. Likely structures for these two additional metabolites, based on these data and on the data obtained for fraction F3 (described below), are presented below.

Glycosyl composition analysis (data not shown) of fraction F3 showed that it contained glycerol and fucose in addition to the expected 2-*O*-methylfucose and *N*-acetylglucosamine. The FAB-MS analysis (Fig. 8A, *inset*) of fraction F3 showed that it consisted of a mixture of six molecules with $(\text{M} + \text{H})^+$ ions at m/z 1473, 1458, 1330, 1316, 1256, and 1213. Tandem MS-MS analysis of each of the six molecular ions was performed. Fig. 8 (A and B) shows the results for the MS-MS analysis of the ions at m/z 1316 and 1473, respectively. The MS-MS results of these and of other molecular ions observed in fraction F3 are summarized in the fragmentation patterns shown in Fig. 8C. The $(\text{M} + \text{H})^+$ molecule at m/z 1501 is from fraction F4 and is discussed further below.

The $(\text{M} + \text{H})^+$ molecule at m/z 1213 has a fragmentation pattern that is consistent with a molecule that has a modified

chitin tetrasaccharide backbone with an *N*-octadecenoyl substituent and in which the reducing *N*-acetylglucosamine has a branching 2-*O*-methylfucosyl residue, *i.e.* NodBj-IV($\text{C}_{18:1}$,MeFuc). The $(\text{M} + \text{H})^+$ molecule at m/z 1256 is 43 atomic mass units greater than that at m/z 1213. This 43-atomic mass unit increase is consistent with an added carbamoyl (Cb) group, as has been reported for the NGR234 and *A. caulinodans* Nod metabolites (13, 45). The fragment ion at m/z 469 would dictate that the carbamoyl group is located on the terminal *N*-octadecenoylglucosamine, indicating that this molecule is NodBj-IV(Cb, $\text{C}_{18:1}$,MeFuc).

The fragmentation pattern of the $(\text{M} + \text{H})^+$ molecule at m/z 1316 supports a structure in which the reducing-end *N*-acetylglucosamine is glycosidically linked to glycerol (loss of 92 atomic mass units to give the ion at m/z 1225) and contains a branching fucosyl residue (loss of 146 atomic mass units to give the ion at m/z 1170). Thus, it is this molecule that accounts for the presence of glycerol and fucose in fraction F3. As with the previous molecule, the fragment ion containing *N*-octadecenoylglucosamine is at m/z 469, indicating that a carbamoyl substituent is located on this residue. These data are consistent with this molecule being NodBj-IV(Cb, $\text{C}_{18:1}$,Fuc,Gro). Also, this molecule is 43 atomic mass units larger than the component of fraction F2 with the $(\text{M} + \text{H})^+$ molecule at m/z 1273 (discussed above), indicating that it is a carbamoylated version of this fraction F2 component. Both $(\text{M} + \text{H})^+$ molecules at m/z 1273

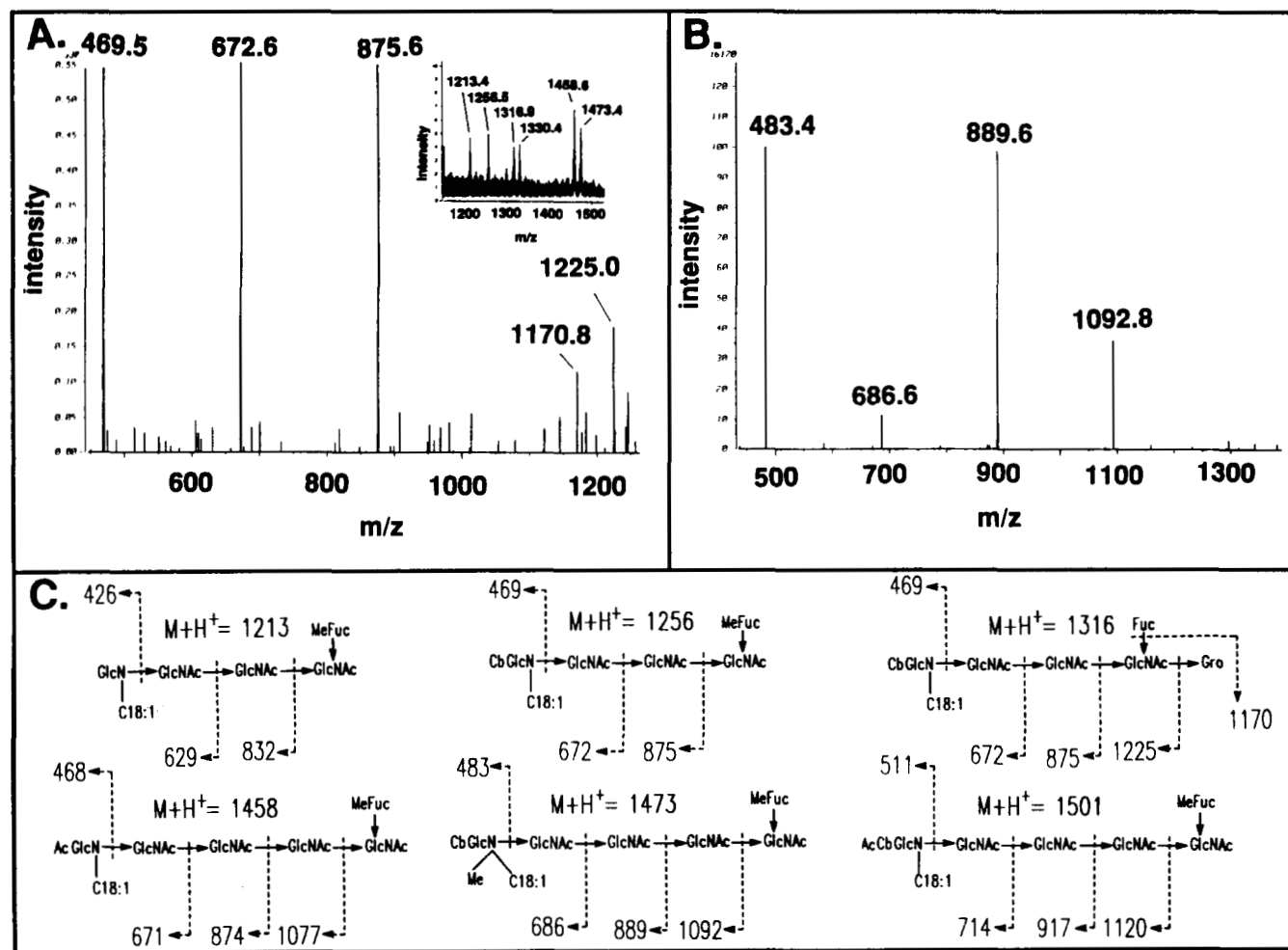


FIG. 8. A, *inset*, FAB-MS spectrum of fraction F3 from *B. japonicum* strain USDA61 revealing that this fraction has six $(\text{M} + \text{H})^+$ molecular ions at m/z 1213.4, 1256.5, 1316.9, 1330.4, 1458.8, and 1473.4; A, MS-MS spectrum of the ion at m/z 1316.9; B, MS-MS spectrum of the ion at m/z 1473.4; C, fragmentation patterns obtained for the above ions as well as for the ions at m/z 1213, 1256, and 1458. The fragmentation pattern for another component found in fraction F4, the $(\text{M} + \text{H})^+$ molecule at m/z 1501, is also shown in C.

and 1316 have fragmentation patterns indicating that their reducing ends have a molecular size of 440 atomic mass units (1272 – 832 and 1315 – 875, respectively). Thus, it is likely the (M + H)⁺ molecule at *m/z* 1273, present in fraction F2, is NodBj-IV(C_{18:1},Fuc,Gro).

The (M + H)⁺ molecule at *m/z* 1330 is 14 atomic mass units larger than the (M + H)⁺ molecule at *m/z* 1316, indicating that it has an added methyl group. Based on the previous reports for the NGR234 and *A. caulinodans* Nod metabolites (13, 45), it was likely that this methyl group was present as an *N*-methyl group on the terminal *N*-acylglucosamine. This was confirmed by methanolysis of fraction F3 in methanolic 1 M HCl at 80 °C, followed by hydrolysis in 4 M HCl at 100 °C for 18 h. The glycosyl residues were reduced and acetylated as described (22). Analysis by GC-MS showed the presence of alditol acetates of both *N*-methylglucosamine and glucosamine. The mass spectrum (data not shown) of the alditol acetate of this *N*-methylglucosamine (with a ²H atom at C-1 due to reduction with NaB²H₄) shows the characteristic primary fragments at *m/z* 374 and 159. In addition, small amounts of glycerol, fucose, and 2-*O*-methylfucose were detected, even though the strong hydrolysis conditions would have destroyed a large percentage of these residues. Thus, the (M + H)⁺ molecule at *m/z* 1330 is NodBj-IV(Cb,C_{18:1},NMe,Fuc,Gro). It should also be noted that this molecule is 43 atomic mass units larger than the minor fraction F2 component of the (M + H)⁺ molecule at *m/z* 1287, indicating that the latter minor component is a non-carbamoylated version of the molecule at *m/z* 1330. Thus, the molecule at *m/z* 1287 can be designated as NodBj-IV(C_{18:1},NMe,Fuc,Gro).

The (M + H)⁺ molecule at *m/z* 1458 has a fragmentation pattern identical to that of NodBj-V(Ac,C_{18:1},MeFuc) found in fraction F2 (described above) and in strain USDA135 (also described above). It is likely that this is residual fraction F2 material that was not completely separated from fraction F3.

The (M + H)⁺ molecule at *m/z* 1473 has a fragmentation pattern (shown in Fig. 8B) that is consistent with that described above for fraction F1 (*m/z* 1416), but with carbamoyl (+43 atomic mass units) and methyl (+14 atomic mass units) groups (one each) added to the terminal *N*-octadecenoylglu-

cosamine, resulting in a fragment ion at *m/z* 483. As described above, the only methylated glucosamine found in fraction F3 was *N*-methylglucosamine, indicating that this molecule has an *N*-methyl group. The location of the carbamoyl group could be at C-3, C-4, or C-6. These data indicate that this molecule is NodBj-V(Cb,C_{18:1},NMe,MeFuc).

The (M + H)⁺ molecule at *m/z* 1501 is found in fraction F4. Its molecular size is 43 atomic mass units larger than NodBj-V(Ac,C_{18:1},MeFuc) ((M + H)⁺ 1458), indicating that it has an added carbamoyl group. The fragment ion at *m/z* 511 dictates that this added carbamoyl group is located on the terminal *N*-octadecenoyl-*O*-acetylglucosamine. If the location of the *O*-acetyl group is at C-6 as described above for the USDA135 metabolite, then the carbamoyl group would be located at C-3 or C-4. These data indicate that this molecule is NodBj-V(Ac,Cb,C_{18:1},MeFuc).

Not enough of fractions F2 and F3 were obtained to perform methylation or NMR analysis; therefore, the linkages and anomeric configurations could not be determined. However, based on the structures for the USDA135 Nod metabolites described above and those previously reported (3, 6–9, 13), it is likely that the *N*-acetylglucosaminosyl residues are β-linked and that the fucosyl and 2-*O*-methylfucosyl residues are α-linked to C-6 of the reducing-end *N*-acetylglucosamine. The location of the carbamoyl group on the terminal *N*-acylglucosamines of these Nod metabolites is not known. Larger amounts of these various metabolites are being purified to confirm these structures and to determine their biological activities.

Biological Activity of *B. japonicum* Nod Metabolites—Previous investigations have shown that *V. sativa* is a useful test plant with respect to its reaction to Nod metabolites in that its root hairs are readily deformed (Had activity) by a broad variety of Nod metabolites (6, 8). Fig. 9 shows that fractions F1–F4 from USDA135 have Had activity on *V. sativa* subsp. *nigra* at nanomolar concentrations. Thus, Had activity on *V. sativa* occurs with these Nod metabolites in which the *N*-acyl substituent can be an *N*-hexadecenoyl, *N*-hexadecanoyl, or *N*-octadecenoyl substituent. In addition, Nod metabolites with or without the *O*-acetyl group were active, indicating that there is

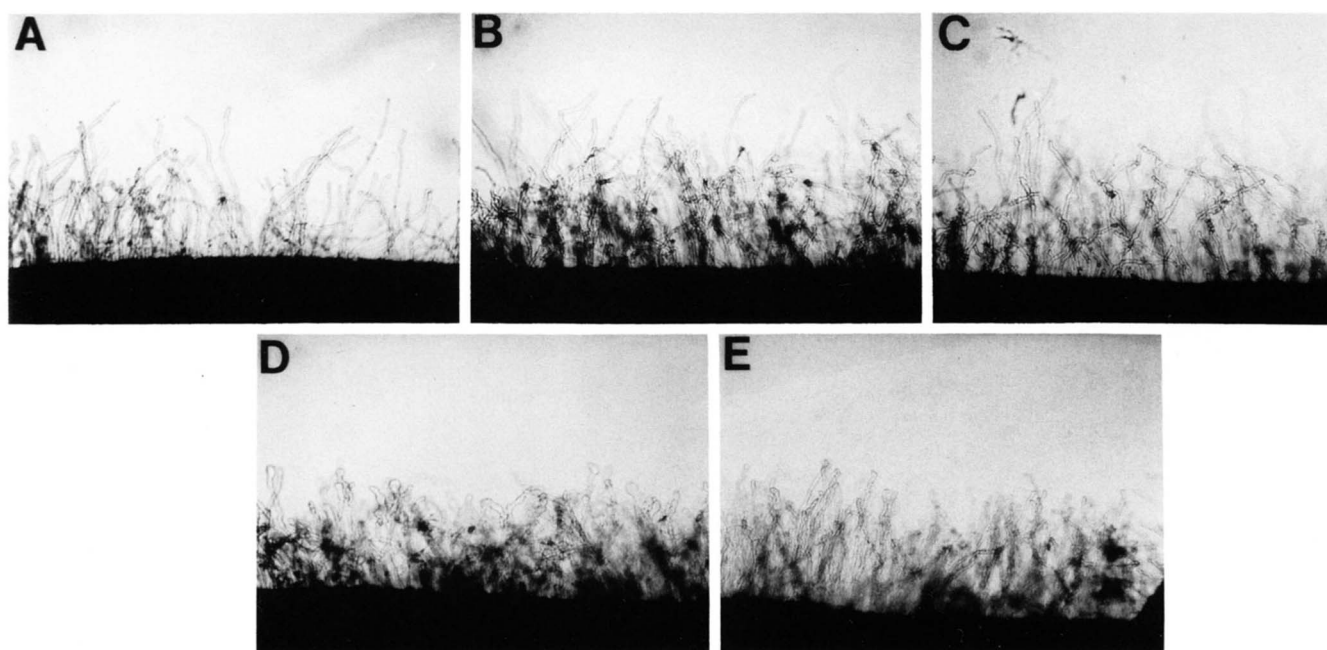


FIG. 9. Root hair deformation activity of fractions F1–F4 (B–E, respectively) on *V. sativa* subsp. *nigra*. A, negative control in which the Nod metabolite was not applied to the root. Compounds were added at a final concentration of 1 ng/ml. Concentrations were determined by integration of the HPLC peaks (see Fig. 2) and comparison with a standard of NodRlv-V(Ac,C_{18:1}).

not an absolute requirement for the *O*-acetyl group for this activity.

A previous paper has shown that NodBj-V(C_{18:1},MeFuc) from strain USDA110 has Had activity on *G. soja* and siratro at 100 pM and no activity on alfalfa even when present at a 10,000-fold higher concentration (7). Under the experimental conditions used, where the entire root was exposed to the Nod metabolite, nodule formation or cortical cell division was not detected on either *G. soja* or siratro. However, using the spot inoculation procedure (see "Experimental Procedures"), outgrowths on the roots of *G. soja* were observed (Fig. 10A). These structures appeared at the point of inoculation with either NodBj-V(C_{18:1},MeFuc) or NodBj-V(Ac,C_{18:1},MeFuc). When 1.5 ng of either compound was applied to the roots, 3 of 12 plants showed one or more of these structures. This ratio increased to 9 of 12 plants when 15 ng was applied. Control plants inoculated with solvent alone did not show any of these structures. The swellings do not show the typical nodule anatomy as they do not contain an internal vascular tissue (data not shown). However, they do not appear to be lateral roots since the methylene blue-stained meristem is not cone-shaped, and it does not originate in the inner cortex as in real lateral roots (Fig. 10B). Closer examination of these Nod metabolite-induced swellings showed them to be very disorganized, with mitotically active cells dispersed near the epidermis. This is similar to soybean nodule development reported by Calvert *et al.* (40), in which initial cell division occurs in the hypodermis. Eventually, some of these structures broke through the epidermis, suggestive of

cell death. In some respects, these structures resembled the popcorn pseudonodules elicited by certain *B. japonicum* mutants that are defective in their lipopolysaccharides (41). It is possible that induction of normal nodule structures requires the presence of additional signals, besides the Nod metabolites, from the bacterium.

DISCUSSION

In this report, we have shown that both Type I and II *B. japonicum* strains produce a variety of Nod metabolites. The structures of these Nod metabolites are summarized in Fig. 11. The types of Nod metabolites produced appear to be strain-dependent. Strain USDA110 produces one major metabolite, NodBj-V(C_{18:1},MeFuc) (7). This strain can also produce lesser amounts of NodBj-V(Ac,C_{18:1},MeFuc) (data not shown). In addition to the USDA110 Nod metabolites, strain USDA135 produces NodBj-V(Ac,C_{18:1},MeFuc), NodBj-V(Ac,C_{16:0},MeFuc), NodBj-V(C_{16:0},MeFuc), and NodBj-V(C_{16:1},MeFuc). All of these factors cause root hair deformation on *V. sativa*. Additionally, both NodBj-V(Ac,C_{18:1},MeFuc) and NodBj-V(C_{18:1},MeFuc) stimulate cell division on *G. soja*. Due to insufficient amounts, the other Nod metabolites from USDA135 have not been tested for their ability to induce cortical cell division.

The Type II strain USDA61 produces eight Nod metabolites in addition to the NodBj-V(C_{18:1},MeFuc) and NodBj-V(Ac,C_{18:1},MeFuc) molecules, which are also produced by the Type I strains. Two of these additional Nod metabolites have chitin pentasaccharide backbones, while the other six have tetrasaccharide backbones. All have an octadecenoyl group as the *N*-acyl substituent. A number of these metabolites have carbamoyl and/or *N*-methyl substituents located on the terminal *N*-octadecenoylglucosamine. In this respect, they are similar to those molecules reported for NGR234 and *A. caulinodans* (13, 45). Four of these metabolites are unique in that the reducing-end *N*-acetylglucosamine contains a branching fucose and is glycosidically linked to glycerol. These four metabolites have tetrasaccharide backbones. This is the first report of Nod metabolites in which the reducing-end *N*-acetylglucosamine does not exist as a free reducing sugar. It is possible that these molecules represent end products with unique biological properties or intermediates in the biosynthesis of these *B. japonicum* Nod metabolites.

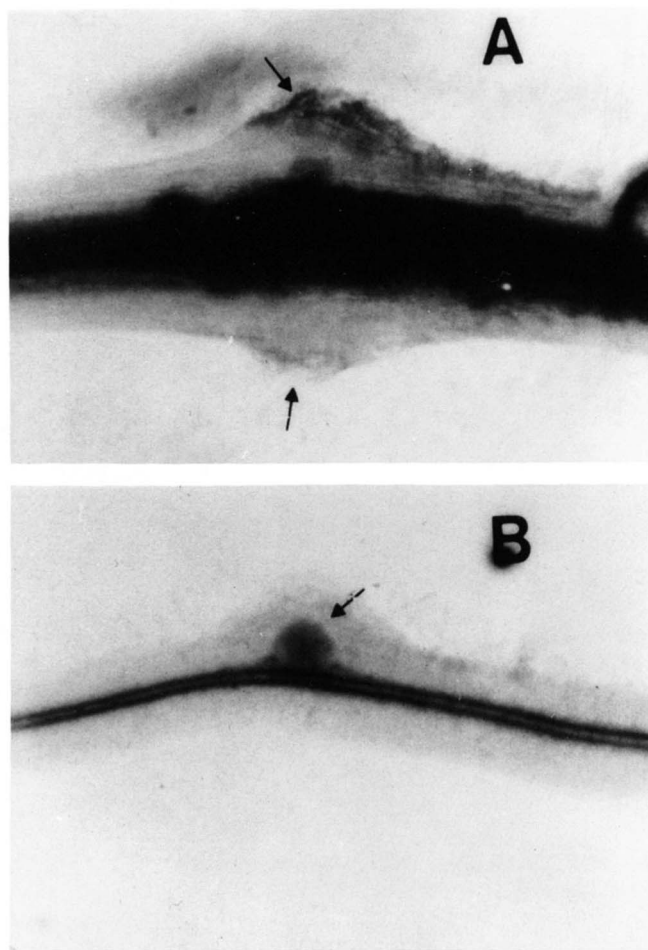
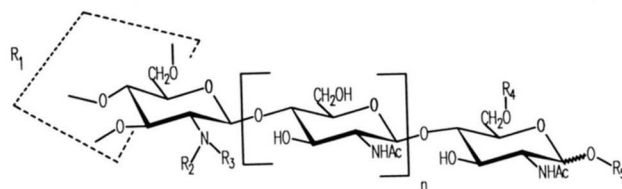


FIG. 10. Formation of root swellings on *G. soja* induced by NodBj-V(C_{18:1},MeFuc). The concentration applied and method of application are described in the text. A, effect of the applied Nod metabolite; B, normal lateral root development.



Nod Metabolite	Strain	R ₁	R ₂	R ₃	R ₄	R ₅	n	(M+H) ⁺
NodBj-V(C _{18:1} ,MeFuc)	110 135 61	H	C _{18:1}	H	2-O-MeFuc	H	3	1416
NodBj-V(Ac,C _{18:1} ,MeFuc)	135 61	Ac	C _{18:1}	H	2-O-MeFuc	H	3	1458
NodBj-V(C _{16:0} ,MeFuc)	135	H	C _{16:0}	H	2-O-MeFuc	H	3	1390
NodBj-V(Ac,C _{16:0} ,MeFuc)	135	Ac	C _{16:0}	H	2-O-MeFuc	H	3	1432
NodBj-V(C _{16:1} ,MeFuc)	135	H	C _{16:1}	H	2-O-MeFuc	H	3	1388
NodBj-V(Cb,C _{18:1} ,NMe,MeFuc)	61	Cb	C _{18:1}	Me	2-O-MeFuc	H	3	1473
NodBj-V(Ac,Cb,C _{18:1} ,MeFuc)	61	Ac,Cb	C _{18:1}	H	2-O-MeFuc	H	3	1501
NodBj-IV(C _{18:1} ,MeFuc)	61	H	C _{18:1}	H	2-O-MeFuc	H	2	1213
NodBj-IV(Cb,C _{18:1} ,MeFuc)	61	Cb	C _{18:1}	H	2-O-MeFuc	H	2	1256
NodBj-IV(C _{18:1} ,Fuc,Gro)	61	H	C _{18:1}	H	Fuc	Gro	2	1273
NodBj-IV(C _{18:1} ,NMe,Fuc,Gro)	61	H	C _{18:1}	Me	Fuc	Gro	2	1287
NodBj-IV(Cb,C _{18:1} ,Fuc,Gro)	61	Cb	C _{18:1}	H	Fuc	Gro	2	1316
NodBj-IV(Cb,C _{18:1} ,NMe,Fuc,Gro)	61	Cb	C _{18:1}	Me	Fuc	Gro	2	1330

FIG. 11. Summary of Nod metabolites from *B. japonicum*. In the case of the R₁ substituent (an acetyl and/or carbamoyl group), the acetyl group of NodBj-V(Ac,C_{18:1},MeFuc) is located at C-6. The location of the carbamoyl group in the various metabolites could be at C-3, C-4, or C-6.

Recently, the structures of several Nod metabolites from the broad host range *Rhizobium* sp. NGR234 have been reported (13). All of these metabolites contain 2-*O*-methylfucose at C-6 of the reducing *N*-acetylglucosamine, while varying in the fatty acyl substituent, *i.e.* either *N*-hexadecanoyl or *N*-octadecenoyl. Other NGR234 Nod metabolites contain carbamoyl groups at C-3, C-4, and/or C-6 of the *N*-methyl-*N*-acetylglucosamine as well as sulfate or acetate at C-3 or C-4, respectively, of the 2-*O*-methylfucosyl residue. Since one of the hosts of NGR234 is soybean, these results would indicate that the 2-*O*-methylfucosyl residue is required for nodulation of soybean. However, another possibility is that the 2-*O*-methylfucosyl residue is important in extending the host range. Both *B. japonicum* and NGR234 have broad host ranges in comparison to *R. leguminosarum* or *R. meliloti*.

That some substituents, such as 2-*O*-methylfucose, carbamoyl, and *N*-methyl groups, may be involved in extending the host range has some support in the literature. Recently, it was reported that *nodS* has homology to methyltransferases that use *S*-adenosylmethionine as the methyl donor (45). It was suggested that this gene is responsible for the *N*-methylation of the *N*-acetylglucosamine of the Nod metabolites (45). When this gene was transferred into *Rhizobium fredii* USDA257, its host range was extended to include *Leucaena*, not normally a host of USDA257 (46). Other reports have shown that mutations in *B. japonicum* genes *nodZ* and *nodVW* result in restriction of the host range, *i.e.* the symbionts no longer nodulate siratro, but still nodulate soybean (47, 48). Examination of the Nod metabolites from a *nodZ*⁻ mutant has shown that they do not contain the 2-*O*-methylfucosyl residue.² Thus, it is possible that certain structural modifications of the Nod metabolites are required for infecting a broad range of hosts.

Further work on the structures and biological activities of Nod metabolites from various *B. japonicum* Type I (16, 42, 43) and II (18, 44) mutants is in progress to determine structure-function relationships of the various host specificity genes.

Acknowledgments—We thank Drs. Kelly Thornburg (Medical University of South Carolina, Charleston, SC) and Ron Orlando (Complex Carbohydrate Research Center) for assistance in obtaining the tandem MS-MS spectra and Dr. Scott Forsberg (Complex Carbohydrate Research Center) for preparing the fatty acid dimethyl disulfide derivative. We also thank Teun Tak for assistance in performing bioassays on *V. sativa* and Dr. Ben Lugtenberg for helpful discussions.

REFERENCES

- Schlaman, H. R. M., Okker, R. J. H., and Lugtenberg, B. J. J. (1992) *J. Bacteriol.* **174**, 5177–5182
- Fisher, R. F., and Long, S. R. (1992) *Nature* **357**, 655–660
- Dénarié, J., and Roche, P. (1992) in *Molecular Signals in Plant-Microbe Communications* (Verma, D. P. S., ed) pp. 295–324, CRC Press, Inc., Boca Raton, FL
- Kosslak, R. M., Bookland, R., Barkei, J., Paaren, H. E., and Appelbaum, E. R. (1987) *Proc. Natl. Acad. Sci. U. S. A.* **84**, 7428–7432
- Smit, G., Puvanesarajah, V., Carlson, R. W., Barbour, W. M., and Stacey, G. (1992) *J. Biol. Chem.* **267**, 310–318
- Spaink, H. P., Sheeley, D. M., van Brussel, A. A. N., Glushka, J., York, W. S., Tak, T., Geiger, O., Kennedy, E. P., Reinhold, V. N., and Lugtenberg, B. J. J. (1991) *Nature* **354**, 125–130
- Sanjuan, J., Carlson, R. W., Spaink, H. P., Bhat, U. R., Barbour, W. M., Glushka, J., and Stacey, G. (1992) *Proc. Natl. Acad. Sci. U. S. A.* **89**, 8789–8793
- Lerouge, P., Roche, P., Faucher, C., Maillet, F., Truchet, G., Promé, J. C., and Dénarié, J. (1990) *Nature* **344**, 781–784
- Schultze, M., Quiclet-Sire, B., Kondorosi, É., Virelizier, H., Glushka, J. N., Endre, G., Géro, S. D., and Kondorosi, A. (1992) *Proc. Natl. Acad. Sci. U. S. A.* **89**, 192–196
- Dénarié, J., Debelle, F., and Rosenberg, C. (1992) *Annu. Rev. Microbiol.* **46**, 497–531
- Roche, P., Lerouge, P., Ponthus, C., and Promé, J.-C. (1991) *J. Biol. Chem.* **266**, 10933–10940
- Kijne, J. W. (1992) in *Biological Nitrogen Fixation* (Stacey, G., Burris, R. H., and Evans, H. J., eds) pp. 349–398, Chapman and Hall Ltd., London
- Price, N. P. J., Relic, B., Talmont, F., Lewin, A., Promé, D., Pueppke, S. G., Maillet, F., Dénarié, J., Promé, J.-C., and Broughton, W. J. (1992) *Mol. Microbiol.* **6**, 3575–3584
- Spaink, H. P., Aarts, A., Stacey, G., Bloemberg, G. V., Lugtenberg, B. J. J., and Kennedy, E. P. (1992) *Mol. Plant Microbe Interact.* **5**, 72–80
- Elkan, G. H. (1992) *Can. J. Microbiol.* **38**, 446–450
- Nieuwkoop, A. J., Banfalvi, Z., Deshmane, N., Gerhold, D., Schell, M. G., Sirotkin, K. M., and Stacey, G. (1987) *J. Bacteriol.* **169**, 2631–2638
- Bergersen, F. J. (1961) *Aust. J. Biol. Sci.* **14**, 349–360
- Stokkermans, T. J. W., Sanjuan, J., Ruan, X., Stacey, G., and Peters, N. K. (1992) *Mol. Plant Microbe Interact.* **5**, 504–512
- Banfalvi, Z., Nieuwkoop, A., Schell, M., Besl, L., and Stacey, G. (1988) *Mol. Gen. Genet.* **214**, 420–424
- Turgeon, B. G., and Bauer, W. D. (1982) *Can. J. Bot.* **60**, 152–161
- Truchet, G., Camut, S., deBilly, F., Odorico, R., and Vasse, J. (1989) *Protoplasma* **149**, 82–88
- York, W. S., Darvill, A. G., McNeil, M., Stevenson, T. T., and Albersheim, P. (1985) *Methods Enzymol.* **118**, 3–40
- Wollenweber, H.-W., and Rietschel, E. Th. (1990) *J. Microbiol. Methods* **11**, 195–211
- Deleted in proof
- Bhat, U. R., and Carlson, R. W. (1992) *Glycobiology* **2**, 535–539
- Yruela, I., Barbe, A., and Grimalt, J. O. (1990) *J. Chromatogr. Sci.* **28**, 421–427
- Piantini, U., Sorensen, O. W., and Ernst, R. R. (1982) *J. Am. Chem. Soc.* **104**, 6800–6801
- Braunschweiler, L., and Ernst, R. R. (1983) *J. Magn. Reson.* **53**, 521–528
- Bax, A., and Davis, D. G. (1985) *J. Magn. Reson.* **65**, 355–360
- Bothner-By, A. A., Stephens, R. L., Lee, J., Warren, C. D., and Jeanloz, R. W. (1984) *J. Am. Chem. Soc.* **106**, 811–813
- Bodenhausen, G., and Ruben, D. J. (1980) *Chem. Phys. Lett.* **69**, 185–186
- Marion, D., and Wuthrich, K. (1983) *Biochem. Biophys. Res. Commun.* **113**, 967–974
- Davis, D. G., and Bax, A. (1985) *J. Am. Chem. Soc.* **107**, 2820–2821
- Griesinger, C., and Ernst, R. R. (1987) *J. Magn. Reson.* **75**, 261–271
- Shaka, A. J., Barker, P. B., and Freeman, R. (1985) *J. Magn. Reson.* **64**, 547–552
- Morris, G. A., and Freeman, R. (1978) *J. Magn. Reson.* **29**, 433–462
- Bodenhausen, G., Freeman, R., and Turner, D. L. (1977) *J. Magn. Reson.* **27**, 511–514
- Demary, M., Puzo, G., and Asselineau, J. (1977) *Nouv. J. Chimie* **2**, 373–378
- Blakeney, A. B., Harris, P. J., Henry, R. J., and Stone, B. A. (1983) *Carbohydr. Res.* **113**, 291–299
- Calvert, H. E., Pence, M. K., Pierce, M., Malik, N. S. A., and Bauer, W. D. (1984) *Can. J. Bot.* **62**, 2375–2384
- Stacey, G., So, J.-S., Roth, L. E., Bhagya Lakshmi, S. K., and Carlson, R. W. (1991) *Mol. Plant Microbe Interact.* **4**, 332–340
- Deshmane, N., and Stacey, G. (1989) *J. Bacteriol.* **171**, 3324–3330
- Sadowsky, M. J., Cregan, P. B., Gottfert, M., Sharma, A., Gerhold, D., Rodriguez-Quinones, F., Keyser, H. H., Hennecke, H., and Stacey, G. (1991) *Proc. Natl. Acad. Sci. U. S. A.* **88**, 637–641
- Ruan, X., and Peters, N. K. (1992) *J. Bacteriol.* **174**, 3467–3473
- Mergaert, P., Van Montagu, M., Promé, J. C., and Holsters, M. (1993) *Proc. Natl. Acad. Sci. U. S. A.* **90**, 1551–1555
- Krishnan, H. B., Lewin, A., Fellay, R., Broughton, W. J., and Pueppke, S. G. (1992) *Mol. Microbiol.* **6**, 3321–3330
- Barbour, W. M., Wang, S.-P., and Stacey, G. (1992) in *Biological Nitrogen Fixation* (Stacey, G., Burris, R. H., and Evans, H. J., eds) pp. 293–348, Chapman and Hall Ltd., London
- Gottfert, M., Grob, P., and Hennecke, H. (1990) *Proc. Natl. Acad. Sci. U. S. A.* **87**, 2630–2684

² G. Stacey, S. Luka, J. Sanjuan, A. J. Nieuwkoop, and R. W. Carlson, submitted for publication.